

## **WATER IN THE EARTH'S MANTLE: MECHANISMS OF HYDROGEN INCORPORATION AND IMPLICATIONS ON MASS AND CHARGE TRANSPORT IN NOMINALLY ANHYDROUS MINERALS**

ALESSANDRO DEL VECCHIO

Dipartimento INGEO Ingegneria e Geologia, Università G. D'Annunzio Chieti-Pescara, Via dei Vestini 31, 66100 Chieti

Experimental studies conducted over the last decades have shown how even small amounts of hydrogen has a large impact on the physical and chemical properties of the Earth's minerals, such as deformation and rheology, seismic velocities, diffusion processes, and electrical conductivities (Mackwell *et al.*, 1988; Mackwell & Kohlstedt, 1990; Kohlstedt & Mackwell, 1998; Poe *et al.*, 2010).

Subduction represents the main mechanism of incorporation and transport of hydrated minerals within the earth, up to the great depth of the transition zone and lower mantle: experimental studies (Peacock, 1990; Williams & Hemley, 2001) have estimated that the content of water transported by subducting plates is about  $8.7 \cdot 10^{11}$  kg/year, whereas quantities of water released in gaseous form is about  $2.0 \cdot 10^{11}$  kg/year; so it is clear that the amount of water re-emitted by degassing processes is much smaller than that subducted.

At high pressures, the water content could be regulated by the presence of DHMS (Dense Hydrous Magnesium Silicates) and, although they have never been observed, these mineralogical phases are stable to certain ranges of pressure and temperature; at greater mantle depths they would undergo a series of phase transitions with a more stable structure, resulting in the release of large quantities of water in the mantle.

The first studies which investigated water in nominally anhydrous minerals (NAMs) were mainly carried out on olivine (Bai & Kohlstedt, 1993; Kohlstedt *et al.*, 1996), pyroxenes (Bell & Rossman, 1992) and garnets (Lu & Keppler, 1997), because they were considered to be the main anhydrous mineral phases present in the mantle.

Regarding water storage capacity, the mantle has a strong heterogeneity: the upper and lower mantle have the possibility of very low storage (< 0.2 wt.%), whereas the transition zone has a storage capacity of about 3 wt.% because of the presence of wadsleyite and ringwoodite, high pressure and high temperature polymorphs of olivine: this means that transition zone could be the largest water reservoir in the Earth (Kohlstedt *et al.*, 1996; Ohtani, 2005).

The aim of this work is to further the understanding of the role of water in olivine; to achieve this aim, hydrous polycrystalline samples of a natural San Carlos olivine and synthetic forsterite were synthesized.

Forsterite was firstly obtained by thermo-mechanical synthesis, derived from a combination of mechanical activation and heat treatment (Tavangarian & Emadi, 2009, 2010). To achieve forsterite stoichiometry, the mechanical treatment was carried out by mixing appropriate amounts of talc ( $\text{Mg}_3\text{Si}_4\text{O}_{10}(\text{OH})_2$ ) and hydroxyl magnesium carbonate ( $\text{MgCO}_3 \cdot \text{Mg}(\text{OH})_2 \cdot \text{H}_2\text{O}$ ) in agate mortar for about 20 minutes, whereas the heat treatment was carried out in a platinum crucible using the Nabertherm LHT 04/18 chamber furnace in the temperature range between 40-1600 °C.

High pressure and high temperature experiments were carried out using a Vöggenreiter  $\frac{3}{4}$  inch end-loaded piston cylinder apparatus and Multi Anvil apparatus at the INGV National Institute of Geophysics and Vulcanology (ROME): 16 synthesis runs were carried out, keeping constant the value of temperature (1000-1100 °C), varying pressure (1-4 GPa) and timing of system block to reach the conditions of pressure and temperature required, and using liquid  $\text{H}_2\text{O}$  and  $\text{D}_2\text{O}$  as hydrogen source.

FTIR spectroscopy is the primary method for the study and identification of hydrogen in nominally anhydrous minerals such as olivine: olivine shows a great complexity of OH defects, and previous studies have identified more than 50 bands (Miller *et al.*, 1987): FTIR spectra were acquired using Bruker Hyperion 3000 Microscope equipped with Global IR source, a KBr broadband beamsplitter, and a liquid nitrogen-cooled MCT

detector coupled with 15X Schwarzschild objective at Laboratori Nazionali di Frascati, Istituto di Fisica Nucleare (INFN) in Frascati (Rome).

For FTIR analyses, sections of capsules from HP and HT syntheses were cut perpendicular to the cylindrical axes using a diamond saw (thickness 0.3 mm) and embedded in an epoxy resin. The sections were thinned and polished to a thickness ranging between 300 and 700 microns. FTIR acquisition was performed at ambient temperature with a nominal resolution of 4 cm<sup>-1</sup> with 64 scans both for spectrum and background.

OH absorption bands (Fig. 1) were observed in the frequency range between 3000 and 4000 cm<sup>-1</sup>, mainly due to phenomena of symmetric and asymmetric stretching of OH groups: within each sample, a square section (40×40 μm) in the image area was identified, choosing a series of points (4-8), spaced about 150 μm apart from each other along the section.

With unoriented single crystals or with polycrystalline samples (as in this study) the water content may be determined using Paterson (1982) calibration: this calibration is usually used in absence of specific calibrations for a particular mineral (Bolfan-Casanova *et al.*, 2000), although it may lead to an underestimation of the water content (Libowitzky & Rossman, 1997). It is based on an empirical correlation between the OH stretching frequency and the extinction coefficient, which leads to the following expression:

$$C_{OH} = \frac{X_i}{150 \xi} \int \frac{H(v)/t}{(3780-v)}$$

where  $C_{OH}$  is the concentration of hydroxyl (H/10<sup>6</sup>Si),  $\xi$  is an orientation factor, equal to 1/3 for non-polarized measurements,  $H(v)/t$  is the absorption coefficient (cm<sup>-1</sup>), and  $X_i$  is the density factor (Table 1).

Table 1 - Major absorption bands, thickness and final OH concentrations from FTIR analysis.

Sample	Thickness (mm)	Major absorption bands (cm <sup>-1</sup> )	C <sub>OH</sub> (wt. ppm H <sub>2</sub> O)	C <sub>OH</sub> (H/10 <sup>6</sup> Si)
H0409	0.515	3476, 3537, 3552, 3566, 3578, 3607, 3610, 3614, 3690, 3697	102 ± 2	1668
H0203	0.580	3476, 3532, 3550, 3566, 3575, 3578, 3604, 3612, 3692, 3698	106 ± 3	1729
D1707	0.732	3476, 3532, 3549, 3566, 3577, 3605, 3612, 3693, 3698	131 ± 2	2136
H1902	0.320	3475, 3531, 3549, 3566, 3578, 3601, 3608, 3612, 3692, 3699	196 ± 4	3194
H0303	0.520	3476, 3528, 3549, 3566, 3576, 3579, 3605, 3612, 3692, 3699	203 ± 4	3323
D1409	0.420	3476, 3531, 3546, 3566, 3574, 3578, 3601, 3611, 3614, 3693, 3699	282 ± 5	4610
H2002	0.381	3474, 3536, 3551, 3566, 3578, 3602, 3611, 3614, 3691, 3699	402 ± 8	6556

This density factor may be expressed by the equation  $X = 18 \cdot 10^6 / \rho$ , where  $\rho$  is the density of the considerate phase (g/cm<sup>3</sup>), and its value is linked to the chemical composition, and is equal to  $4.390 \cdot 10^4$  H/10<sup>6</sup>Si or 2695 ppm H<sub>2</sub>O for olivine (Mg<sub>0.9</sub>Fe<sub>0.1</sub>)SiO<sub>4</sub> and  $4.366 \cdot 10^4$  H/10<sup>6</sup>Si or 793 ppm H<sub>2</sub>O for forsterite Mg<sub>2</sub>SiO<sub>4</sub>.

An early study (Bai & Kohlstedt, 1993) divided the OH stretching region of the olivine FTIR spectrum into two main groups: group I includes bands in a frequency range between 3450-3650 cm<sup>-1</sup> whereas group II includes vibrational modes in a frequency range between 3200-3450 cm<sup>-1</sup>. The presence of these two distinct

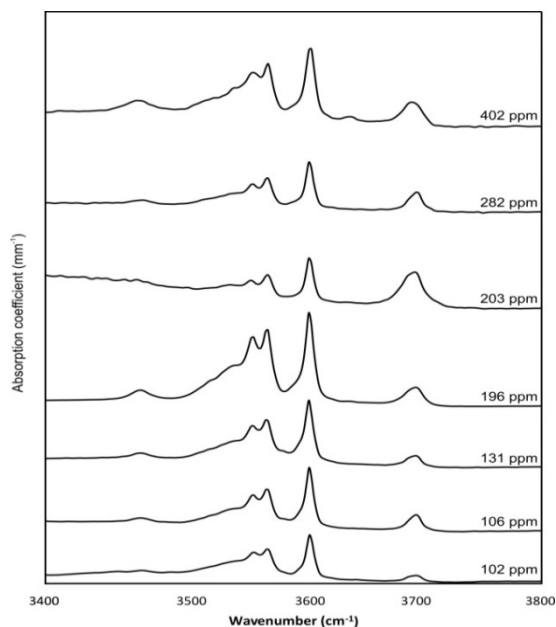


Fig. 1 - FTIR spectra of <sup>1</sup>H hydrous samples.

absorption bands therefore indicates that hydrogen is associated with two different types of lattice sites, doubly charged or single charged interstitial ions.

More recent studies (Lemaire *et al.*, 2004; Kovacs *et al.*, 2010) assigned the two OH stretching regions previously identified among four main incorporation mechanisms of hydrogen in olivine as: *i*) silicate vacancies: *ii*) magnesium vacancies, *iii*) titanoclinohumite defects, and *iv*) trivalent cations defects. Even more recently, other studies (Balan *et al.*, 2011, 2014; Ingrin *et al.*, 2013) have also proposed the contribution of OH in interstitial position defects.

Among these various possible defect sites, considering the chemical composition of the starting materials, in this study we first took into account the silicate defect often referred to as “hydrogarnet defect” considered to be very common: four protons charge balance a silicate vacancy in a tetrahedral site, leading to a stoichiometry of  $\text{Mg}_2\text{H}_4\text{O}_4$  (Lemaire *et al.*, 2004, Kovacs *et al.*, 2010). A subsequent study (Balan *et al.*, 2011) took into account four different models (Si\_1, Si\_2, Si\_3, and Si\_4), depending on the position of the protons in the crystal lattice of olivine, leading to different vibrational modes in a frequency range between 3400-3700  $\text{cm}^{-1}$  (Si\_1 about 3600  $\text{cm}^{-1}$ , Si\_2 3450-3700  $\text{cm}^{-1}$ , Si\_3 3500-3600  $\text{cm}^{-1}$  and Si\_4 3400-3600  $\text{cm}^{-1}$ ).

Another major hydrogen incorporation mechanism involves the substitution of divalent cations (usually Mg) by two protons, leading to a final stoichiometry of  $\text{MgH}_2\text{SiO}_4$ . Specific studies provided important information on the structure of doubly protonated magnesium vacancies (Balan *et al.*, 2011) that result in two vibrational modes, involving the coupled movement of OH groups. Both of these modes are observed at significantly lower frequencies compared to the Si vacancy incorporation mechanism: a vibrational mode at 3225  $\text{cm}^{-1}$  corresponds to the stretching phase of OH groups, with a strong IR activity and strongly polarized along the *c* axis, whereas the vibrational mode at 3212  $\text{cm}^{-1}$  corresponds to a weaker and slightly phase-shifted mode.

A further mechanism of hydrogen incorporation in olivine/forsterite is linked to the presence of hydrogen ions in interstitial positions, where hydrogen atom resides outside of either a normal T or M lattice position (Ingrin *et al.*, 2013), leading to two main IR bands, at frequencies of 3566 and 3617  $\text{cm}^{-1}$  (Lemaire *et al.*, 2004, Ingrin *et al.*, 2013, Balan *et al.*, 2014). Two main configurations are hypothesized for the incorporation of OH groups in interstitial position: in the first configuration, called OH<sub>a</sub>, the hydrogen atom points towards the near M1 chain, whereas in the second configuration OH<sub>b</sub>, it points towards the Si tetrahedral site.

Fits of our FTIR spectra were carried out using Lorentzian lineshapes in the frequency range containing absorption bands due to OH stretching vibrations. Spectra of our samples containing  $^1\text{H}$  all showed a series of peaks in a frequency range between 3400-3800  $\text{cm}^{-1}$  (Table 1), indicative of the Si\_vacancy mechanism of hydrogen incorporation.

More specifically, the observed peak positions and their relative absorbances allowed us to assign the vibrational modes to the Si\_2 and Si\_3 configurations (Fig. 2). According to Balan *et al.* (2011) in the Si\_2 vacancy, while the O<sub>1</sub>-H group points towards the center of the tetrahedron or along one of the tetrahedral bridges, the other three groups point out of the tetrahedron into the empty octahedral sites, whereas in Si\_3 one of the OH groups points towards an empty site.

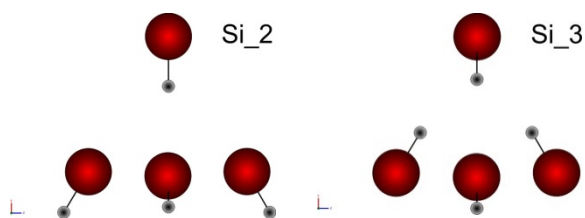


Fig. 2 - Structural models of Si\_2 and Si\_3 vacancies, with oxygen (red) and hydrogen (grey).

Differences of the order of 6-10  $\text{cm}^{-1}$  are observed between the peaks in this study compared to Lemaire *et al.* (2004), Kovacs *et al.* (2010), and Balan *et al.* (2011). These differences might indicate different orientations of the H-species in these defects sites, but the absence of vibrational modes below 3400  $\text{cm}^{-1}$  was a clear sign that hydrogen avoids the incorporation mechanism related to the magnesium vacancies in our samples.

Furthermore, additional vibrational modes related to the interstitial OH position were identified, mainly in the OH1a configuration ( $3566\text{ cm}^{-1}$ ), but also to the OH1b configuration ( $3610\text{-}3617\text{ cm}^{-1}$  peaks).

The results in terms of water content, both in wt.% and in H/Si ratio, and positions of the major absorption bands are summarized in Table 1.

The presence of  $\text{Si}_{\text{i}}$  vacancy and interstitial vacancy lead to two principal observations:

- during the preparation of the HP-HT synthesis, no additional silicate phase was added to buffer the silica activity of the forsterite/olivine, leading to the main incorporation mechanism of  $\text{Si}_{\text{i}}$  vacancy (Kovacs *et al.*, 2010);
- the XRPD analysis of starting materials showed that, together with forsterite, the sample F2509 contained traces of MgO periclase that likely buffered MgO activity; all analyzed spectra, in fact, did not show any vibrational mode in the frequency range below  $3400\text{ cm}^{-1}$ .

Using the same starting materials substituting the same volume of  $\text{D}_2\text{O}$  in place of  $\text{H}_2\text{O}$ , our goal was to produce samples, with similar if not equal final concentrations of dissolved  $\text{D}_2\text{O}$  as those containing  $\text{H}_2\text{O}$ , in order to be used for subsequent hydrogen self-diffusion experiments. It is important to clarify that there are currently no studies of the hydration of nominally anhydrous minerals with deuterium and, in particular, olivine. Thus, our data acquired standardless, cannot be compared with previous studies, as there are currently no FTIR spectra of  $\text{D}_2\text{O}$ -doped olivine.

All our FTIR spectra (Fig. 3) show that deuterium is undetectable, yet small concentrations of hydrogen manage to contaminate the synthesis, leading to a broad peak in the OH stretching frequency range. We

hypothesize that an interaction was allowed between liquid  $\text{D}_2\text{O}$  and the external environment during the preparation of the experiment (either during the loading of liquid  $\text{D}_2\text{O}$  into the capsule or during the welding process), during which fast chemical exchange between atmospheric  $^1\text{H}$  and  $^2\text{H}$  in the liquid occurred. If the starting material contained both  $\text{H}_2\text{O}$  and  $\text{D}_2\text{O}$ , we then surmised that olivine preferentially incorporated  $\text{H}_2\text{O}$  rather than  $\text{D}_2\text{O}$  because we were unable to observe in our spectra any vibrational modes in the O-D frequency region. Interestingly, applying the Paterson (1982) calibration to estimate total water concentration, we observed equal if not greater concentrations of dissolved  $\text{H}_2\text{O}$  in these samples even though the only spectral features in the OH stretching region was a weak but very broad absorption band at about  $3500\text{ cm}^{-1}$ .

Du Frane & Tyburczy (2012) carried out a series of exchange experiments between hydrogen and deuterium in olivine using different techniques than our study. In order to obtain FTIR spectra of deuterium in olivine to compare with our results, the sample PC30 from their study were also analyzed: FTIR spectra of the PC30 sample were carried out at the INFN Laboratory of Frascati using a FPA (Focal Plane Array) of a

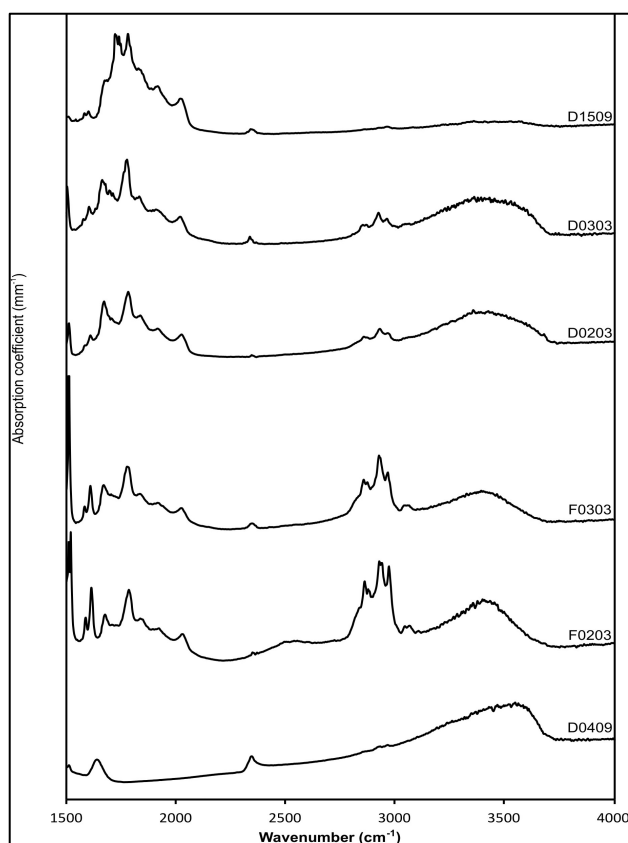


Fig. 3 -FTIR spectra of  $^2\text{H}$  hydrous samples.

liquid nitrogen-cooled MCT detectors coupled with 15X Schwarzschild objective, allowing us to obtain a total coverage of the sample, giving the possibility to observe a FTIR spectrum at a spatial resolution of a single pixel of the image (Fig. 4).

FTIR analyses on Sample PC30 showed that, even if the presence of deuterium through SIMS analysis was observed, any absorption features at frequencies near  $2600\text{ cm}^{-1}$  were present where OD stretching modes should occur.

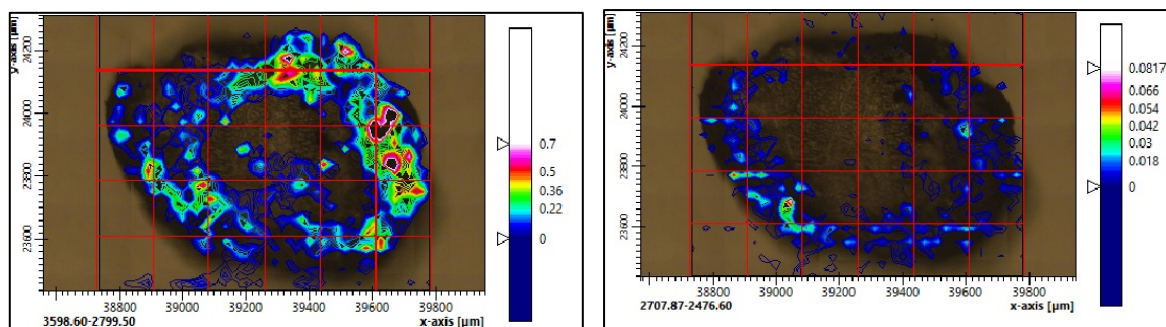


Fig. 4 - FPA image and integrated area in frequency range  $2400\text{--}2700\text{ cm}^{-1}$  (right) and  $2800\text{--}3600\text{ cm}^{-1}$  (left).

FTIR spectroscopy is particularly advantageous for the study of volatile diffusion in minerals because it allows to analyze larger sections of the sample, with a spatial resolution equal and, in some cases, greater than that of the SIMS analyses. Furthermore, the use of special types of detectors, such as FPA, allows the determination of both the concentration and speciation of volatile components over very large sample areas, leading to both a quantitative and qualitative analysis of the diffusion process. SIMS, on the other hand, may be more sensitive to smaller concentrations of the volatile element, but cannot distinguish among the various lattice sites in which it resides.

To understand the kinetics of the H-D exchange process occurring between the atmosphere and liquid added to the capsule under the ambient conditions of the laboratory, we acquired FTIR spectra of a liquid  $\text{D}_2\text{O}$  droplet deposited on the diamond mount of an attenuated total reflectance (ATR) module exposed to the laboratory atmosphere. Approximately the same volume of  $\text{D}_2\text{O}$  liquid used in our high-pressure experiments was used for the ATR measurements.

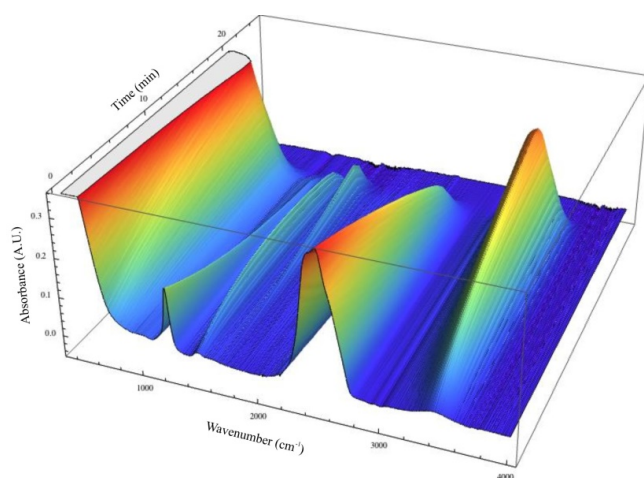


Fig. 5 - Total FTIR spectra for  $^1\text{H}\text{--}^2\text{H}$  exchange process.

Spectra were acquired every 60 seconds over the frequency range  $1000\text{--}4000\text{ cm}^{-1}$ , so that all DOD, DOH and HOH bending, as well as OD and OH stretching vibrational modes might be observed. The gradual exchange of H for D was monitored for approximately 25 minutes, until droplet evaporated entirely, as verified by a spectrum void of any peaks.

The Fig. 5 evidence the whole range acquisition of FTIR spectra showing at the onset of the exchange process the two main peaks due to D-O-D bending ( $1250\text{ cm}^{-1}$ ) and OD stretching ( $2500\text{ cm}^{-1}$ ). With increasing time, these two bands become increasingly more symmetric and two new

peaks appear almost immediately at  $1500\text{ cm}^{-1}$  (DOH bending) and  $3600\text{ cm}^{-1}$  (OH stretching) and their intensities continue to increase with time at the expense of the DOD and OD bands.

After approximately 10 minutes the HOH bending vibrational mode appears at about  $1650\text{ cm}^{-1}$  and its intensity increases until the sample has completely evaporated.

This preliminary study of isotopic exchange process between hydrogen and deuterium could be explained by a structural model of liquid water based on different domains distinguished by varying degrees of order. The notable change of the OD stretching band from asymmetric to symmetric with increasing time might be the result of H preferentially substituting for D in specific domains during the initial stages of exchange. After its incorporation into the liquid phase the diffusion process allowed hydrogen to exchange for deuterium in other domains.

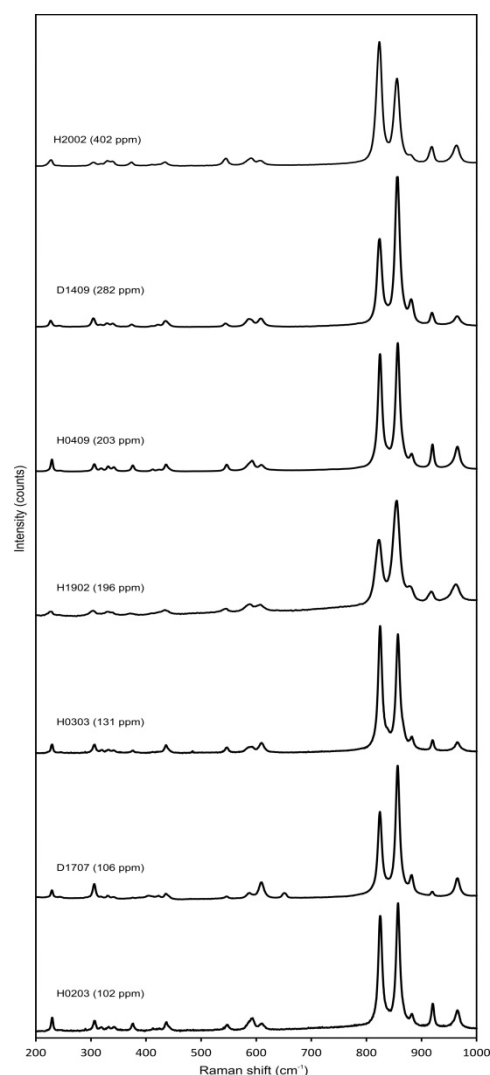


Fig. 6 - Raman spectra of hydrous samples.

effects without knowledge of the grain orientations at which spectra were acquired on our polycrystalline samples.

The incorporation of hydroxyl groups led also to a variation in the number of peaks observed in the Raman spectrum. Both in the lower and higher frequency regions, a new series of peaks were detectable, which had to be associated with vibrational modes involving the motion of OH groups.

Raman spectroscopy was primarily used to understand how water may influence crystal structure of minerals; since Raman spectroscopy is complementary to FTIR spectroscopy, it allowed us to obtain important information about the strength of Si-O bonds in the tetrahedral structure, as well as to understand the interaction between tetrahedral and octahedral cations.

The same samples used for FTIR analysis were also analyzed by Raman spectroscopy between  $100\text{-}1200\text{ cm}^{-1}$  (Fig. 6) at the Volcanology and Experimental Petrology Laboratory of the University of Roma 3, in order to study the effect of water on the vibrational modes of forsterite and olivine. The Horiba Raman LabRam HR spectrometer is equipped with a green laser ( $532\text{ nm}$  wavelength,  $50\text{ mW}$  power), and random measurement points were chosen through a  $100\times$  objective. We used a  $1800\text{ grooves/mm}$  ( $1\text{ cm}^{-1}$  resolution) monochromator grating, with typical acquisition times on the order of  $30\text{-}60\text{ s}$  and  $10\text{-}15$  accumulations for each spectrum.

The analysis of Raman spectra were focused first on the variations of peaks positions (frequency) of the internal modes, such as the  $965$ ,  $856$ ,  $824$ ,  $608$ ,  $545$  and  $422\text{ cm}^{-1}$  vibrational modes observed in an anhydrous San Carlos olivine specimen; comparison of our data with previous studies (Chopelas, 1991; Kolesov & Geiger, 2004; McKeown *et al.*, 2010) showed a more than acceptable reliability of the acquired data.

With regard to intensity variations, it was showed that relative intensity variations among the five principal Raman bands in the high frequency region were strongly coupled to crystallographic orientation of the olivine grain with respect to the incident unpolarized laser radiation (Ishibashi *et al.*, 2008). Although the presence of dissolved  $\text{H}_2\text{O}$  in olivine should also affect band intensities if hydrogen preferentially occupies certain defect sites, it would be difficult to separate the two

At higher frequencies, peaks at 882 and 921  $\text{cm}^{-1}$  were detected: in previous studies (Kolesov & Geiger, 2004) these peaks were attributed to  $B_{3g}$  vibrational modes of forsterite, but other authors (Chopelas, 1991) did not observe these peaks in the experimental data. At lower frequencies, new peaks might be related to the formation of new bonds between  $\text{Mg}^{2+}/\text{Fe}^{2+}$  cations and  $\text{OH}^-$  groups.

Crystal structures of forsterite and olivine are characterized by densely packed isolated  $\text{SiO}_4$  tetrahedra having strong Si-O bonds, which may account for the low solubilities of these minerals.

With increasing water concentration it is increasingly more likely that defect sites contain more than one proton on average. The presence of new vibrational modes at high frequency means that hydrogen is more associated with the Si-O bonds of the tetrahedral unit, leading to variations of the Raman spectrum of olivine.

High-Pressure and High-Temperature laboratory methods, of such as the piston cylinder and multianvil apparatus, allowed us to study and recreate conditions occurring at hundreds of kilometer depths in the mantle.

The use of polycrystalline samples as starting materials, along with a fluid phase as a hydrogen source, allowed to provide comparable results with other experimental data in the literature.

However, we found that standard experimental methods are limited in their effectiveness regarding H/D isotopic substitution in nominally anhydrous minerals, suggesting that improvements are still needed.

FTIR spectroscopy was proved to be a highly efficient method to investigate the presence, the concentration, and the speciation of hydrogen in nominally anhydrous minerals; the results obtained showed that the hydration process of minerals using  $^1\text{H}$  as hydrogen source leads to final concentrations between 100-500 ppm  $\text{H}_2\text{O}$ , allowing us to understand the main mechanisms of hydrogen incorporation which, without the presence of a minor pyroxene phase to buffer silica, occur via Si vacancies associated with interstitial defects in the crystal lattices, corresponding to vibrational modes located in the frequency range between 3400-3700  $\text{cm}^{-1}$  (3549, 3566, 3578, 3611, 3699  $\text{cm}^{-1}$  as main peaks).

The deuteration process of olivine proved to be the most innovative and experimentally challenging aspect of this PhD thesis: the results obtained showed that given the low  $\text{H}_2\text{O}$  solubility in olivine,  $\text{D}_2\text{O}$  is even more difficult to incorporate into its structure at high pressures and temperatures at which conditions are more favorable.

Raman spectroscopy allowed us to observe how the presence of water in the crystal lattices may influence the physical and chemical characteristics of the studied minerals. Hydrogen led to a weakening of olivine crystal structure, even within in the tetrahedral  $\text{SiO}_4$  group, with intensity inversions observed for the main peaks at 824, 856 and 965  $\text{cm}^{-1}$ ; moreover, systematic changes were also noted linked to the octahedral structures of Fe and Mg at lower frequencies.

The incorporation of hydrogen led to a series of variations in vibrational features of forsterite and olivine; protons interact with the apical oxygen of  $\text{SiO}_4$  groups, showing changes in the number of peaks and in the values of frequencies and intensities of the main vibrational modes of olivine.

In conclusion, the high precision, accuracy and attention required in the preparation of this experimental study will be a new starting point for the development of increasingly more sophisticated techniques that benefit the study of the physical and chemical characteristics of mantle minerals at great depths, with particular attention to the roles of  $\text{H}_2\text{O}$  and other volatile components.

Water plays a key role in the field of experimental mineralogy and petrology; recent studies (Pearson *et al.*, 2014) on  $\text{H}_2\text{O}$ -bearing silicate phases found in natural diamonds give us the confirmation that water is present at great depths in the innermost regions of the Earth. This means that results from this study and from new studies to come should contribute to the understanding of how the presence of water in nominally anhydrous minerals may affect the dynamics of the deep Earth.

## REFERENCES

- Bai, Q. & Kohlstedt, D.L. (1993): Effects of chemical environment on the solubility and incorporation mechanism for hydrogen in olivine. *Phys. Chem. Miner.*, **19**, 460-471.

- Balan, E., Ingrin, J., Delattre, S., Kovacs, I., Blanchard, M. (2011): Theoretical infrared spectrum of OH-defects in forsterite. *Eur. J. Mineral.*, **23**, 285-292.
- Balan, E., Blanchard, M., Lazzeri, M., Ingrin, J. (2014): Contribution of interstitial OH groups for the incorporation of water in forsterite. *Phys. Chem. Miner.*, **41**, 105-114.
- Bell, D.R. & Rossman G.R. (1992): Water in Earth's mantle: the role of nominally anhydrous minerals. *Science*, **225**, 1391-1397.
- Bolfan-Casanova, N., Keppler, H., Rubie, D.C. (2000): Water partitioning between nominally anhydrous minerals in the MgO-SiO<sub>2</sub>-H<sub>2</sub>O system up to 24 GPa: implications for the distribution of water in the Earth's mantle. *Earth Planet. Sci. Lett.*, **182**, 209-221.
- Chopelas, A. (1991): Single crystal Raman spectra of forsterite, fayalite and monticellite. *Am. Mineral.*, **76**, 1101-1109.
- Du Frane, W.L. & Tyburczy, J.A. (2012): Deuterium-hydrogen exchange in olivine: implications for point defects and electrical conductivity. *Geochem. Geophys. Geosy.*, **13**(3), Q03004, doi:10.1029/2011GC003895.
- Ingrin, J., Liu, J., Depecker, C., Kohn, S.C., Balan, E., Grant, K.J. (2013): Low-temperature evolution of OH bands in synthetic forsterite, implication for the nature of H defects at high pressure. *Phys. Chem. Miner.*, **40**, 449-510
- Ishibashi, H., Arakawa, M., Ohi, S., Yamamoto, J., Miyake, A., Kagi, H. (2008): Relationship between Raman spectral pattern and crystallographic orientation of a rock-forming mineral: a case study of Fo<sub>89</sub>Fa<sub>11</sub> olivine. *J. Raman Spectrosc.*, **39**, 1653-1659.
- Kohlstedt, D.L. & Mackwell, S.J. (1998): Diffusion of hydrogen and intrinsic point defects in olivine. *Z. Phys. Chem.*, **207**, 147-162.
- Kohlstedt, D.L., Keppler, H., Rubie, D.C. (1996): Solubility of water in the  $\alpha$ ,  $\beta$  and  $\gamma$  phases of (Mg,Fe)<sub>2</sub>SiO<sub>4</sub>. *Contrib. Mineral. Petr.*, **123**, 345-357.
- Kolesov, B.A. & Geiger, C.A. (2004): A Raman spectroscopic study of Fe-Mg olivines. *Phys. Chem. Miner.*, **31**, 142-154.
- Kovacs, I., O'Neill, H.S., Hermann, J., Hauri, E.H. (2010): Site-specific O-H absorption coefficients for water substitution into olivine. *Am. Mineral.*, **95**, 292-299.
- Lemaire, C., Kohn, S.C., Brooker, R.A. (2004): The effect of silica activity on the incorporation mechanisms of water in synthetic forsterite: a polarized infrared spectroscopic study. *Contrib. Mineral. Petr.*, **147**, 48-57.
- Libowitzky, E. & Rossman, G.R. (1997): An IR absorption calibration for water in minerals. *Am. Mineral.*, **82**, 1111-1115.
- Lu, R. & Keppler, H. (1997): Water solubility in pyrope to 100 kbar. *Contrib. Mineral. Petr.*, **129**, 35-42.
- Mackwell, S.J. & Kohlstedt, D.L. (1990): Diffusion of hydrogen in olivine: implications for water in the mantle. *J. Geophys. Res.*, **95**, 5079-5088.
- Mackwell, S.J., Dimos, D., Kohlstedt, D.L. (1988): Transient creep of olivine: point defect relaxation times. *Philos. Mag.*, **57**, 779-789.
- McKeown, D.A., Bell, M.I., Caracas, R. (2010): Theoretical determination of the Raman spectra of single-crystal forsterite (Mg<sub>2</sub>SiO<sub>4</sub>). *Am. Mineral.*, **95**, 980-986.
- Miller, G., Rossman, G.R., Harlow, G.E. (1987): The natural occurrence of hydroxide in olivine. *Phys. Chem. Miner.*, **14**, 461-472.
- Ohtani, E. (2005): Water in the mantle. *Elements*, **1**, 25-30.
- Paterson, M.S. (1982): The determination of hydroxyl by infrared absorption in quartz, silicate glasses and similar materials. *Bull. Mineral.*, **105**, 20-29.
- Peacock, S.M. (1990): Fluid processes in subduction zones. *Science*, **248**, 329-337.
- Pearson, D.G., Brenker, F.E., Nestola, F., McNeill, J., Nasdala, L., Hutchinson, M.T., Matveev, S., Mather, K., Silversmit, G., Schmitz, S., Vekemans, B., Vincze, L. (2014): Hydrous mantle transition zone indicated by ringwoodite included in diamond. *Nature*, **507**, 221-224.
- Poe, B.T., Romano, C., Nestola, F., Smyth, J.R. (2010): Electrical conductivity anisotropy of dry and hydrous olivine at 8 GPa. *Phys. Earth Planet. In.*, **181**, 103-111.
- Tavangarian, F. & Emadi, R. (2009): Mechanical activation assisted synthesis of pure nanocrystalline forsterite powder. *J. Alloy. Compd.*, **485**, 648-652.
- Tavangarian, F. & Emadi, R. (2010): Synthesis of pure nanocrystalline magnesium silicate powder. *Ceramics*, **54**, 122-127.
- Williams, Q. & Hemley, R.J. (2001): Hydrogen in the deep earth. *Annu. Rev. Earth Pl. Sc.*, **29**, 365-418.